Spectroscopic factors from the 51V(d,3He)50Ti reaction

Nuclear Physics **A477** (1988) 55–76
North-Holland, Amsterdam

SPECTROSCOPIC FACTORS FROM THE ^{51}V(d, ^{3}He)^{50}Ti REACTION

G.J. KRAMER[1], H.P. BLOK and J.F.A. VAN HIENEN

Natuurkundig Laboratorium, Vrije Universiteit, 1081 HV Amsterdam, The Netherlands

S. BRANDENBURG, M.N. HARAKEH[2] and S.Y. VAN DER WERF

Kernfysisch Versneller Instituut der Rijksuniversiteit, 9747 AA Groningen, The Netherlands

P.W.M. GLAUDEMANS and A.A. WOLTERS

Fysisch Laboratorium, Rijksuniversiteit Utrecht, 3508 TA Utrecht, The Netherlands

Received 2 September 1986
(Revised 25 August 1987)

Abstract: The ^{51}V(d, ^{3}He)^{50}Ti reaction was studied at $E_d = 52.9$ MeV with an energy resolution of about 25 keV. The differential cross sections were compared with DWBA calculations. Up to 7 MeV excitation energy, 33 levels were found corresponding to $l = 3$, $l = 0$ and $l = 2$ pick-up. In addition three possible $l = 1$ transitions were observed. Realistic uncertainties to be assigned to extracted spectroscopic factors were determined by investigating the influence of different optical models, finite-range effects and different prescriptions for the bound-state wavefunction. In one of these prescriptions, electron-scattering data were used to reduce the uncertainty related to the rms radius of the bound-state wavefunction in the DWBA calculations. The experimental results are compared with the theoretical estimates.

E

NUCLEAR REACTIONS ^{51}V(d, ^{3}He), $E = 52.9$ MeV; measured $\sigma(E(^{3}\text{He}), \theta)$. ^{50}Ti deduced levels, L, spectroscopic factors.

1. Introduction

In the past 25 years the (d, ^{3}He) reaction has been used extensively to obtain spectroscopic factors and occupation probabilities for proton orbitals in the ground state of the target nucleus. The spectroscopic factors obtained from the (d, ^{3}He) reaction by comparing measured cross sections to DWBA predictions, depend strongly on the parameters of the bound-state wavefunction (BSWF), the optical potentials, and also on finite-range and non-locality corrections used in the DWBA calculations. Recently high resolution (e, e'p) data have become available [1]). From these data absolute spectroscopic factors can in principle be obtained, since the analysis is independent of the BSWF and the proton optical potential is relatively

[1] Present address: NIKHEF-K, P.O. Box 4395, 1009 AJ Amsterdam, The Netherlands.
[2] Present address: Natuurkundig Laboratorium, Vrije Universiteit, 1081 HV Amsterdam, The Netherlands.

well known. This yields the opportunity to compare the spectroscopic factors obtained from the (d, ^{3}He) reaction with those from the (e, e'p) reaction. An interesting case leading to several well-separated levels up to reasonably high excitation energies is the ^{51}V(e, e'p)^{50}Ti reaction.

It is the purpose of the present paper to obtain spectroscopic information using the (d, ^{3}He) reaction not only for the lowest quadruplet of states, which have been studied [2-5]) extensively in the past, but also for the states higher up in excitation energy. This can also serve the purpose of comparing with the results from the (e, e'p) reaction. Earlier experimental work and analysis were either restricted [2,3,6]) to the lowest quadruplet of states or lacked the adequate resolution (e.g. the ^{51}V(d, ^{3}He)^{50}Ti data from earlier work [2,3]) were obtained with a resolution of ~200 keV) to yield also unambiguous spectroscopic information for higher-lying states. We therefore remeasured the differential cross sections for the various levels populated in this reaction with a resolution of about 25 keV. This resolution is not only good enough to enable a meaningful comparison with the data from the (e, e'p) reaction, but will also be useful in clarifying some ambiguities in the analysis [1]) of the (e, e'p) data, which were taken with a resolution of about 125 keV. Furthermore, a large basis shell-model calculation has been performed to investigate the observed depletion of the $1f_{7/2}$ strength as compared with the simple shell model.

2. Experimental procedure

The experiment was performed at the KVI in Groningen. Momentum-analysed deuterons of 52.9 MeV energy from the AVF cyclotron were used to bombard a self-supporting natural vanadium foil (^{51}V abundance: 99.7%) of 180 μg/cm^2 thickness. The outgoing ^{3}He particles were detected in the focal plane of the QMG/2 magnetic spectrograph [7]). The detection system [8]) consists of two position-sensitive detectors (psd) and a plastic scintillator. The psd's are a combination of a vertical drift chamber and a horizontal resistive-wire proportional counter. The position is determined from the left and right signals of the resistive wire by charge division. An event consists of 8 signals, left and right signals from each of the resistive wires plus the vertical drift-time of each psd, an energy signal from the scintillator and a time-of-flight signal started by the scintillator and stopped by the cyclotron RF signal. During the experiment all events were written to tape for off-line analysis. A rough particle identification was made on-line for monitoring purposes. A very good particle identification was obtained by setting two-dimensional gates in the two-dimensional scatter plot of the scintillator-energy signal versus the position in the front detector. In this way the overwhelming background of low-energy deuterons could be completely suppressed. This is illustrated in fig. 1. In fig. 2 we show spectra taken at $\theta_{lab} = 4°$, 11° and 17°, which correspond approximately to maxima in the angular distributions of $l = 0$, $l = 2$ and $l = 3$ transfer, respectively. The overall energy resolution was about 25 keV FWHM.

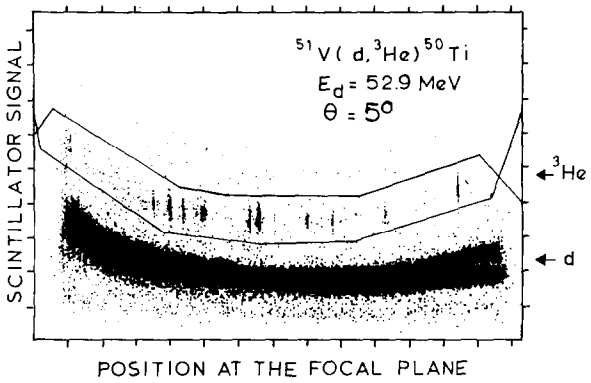

Fig. 1. Two-dimensional scatter plot of the scintillator energy output versus the position in the focal plane of the spectrograph.

The analysis of the spectra was performed with the peak-fitting code SPECFIT [9]). Up to $E_x = 7$ MeV we found 36 levels (see sect. 4, table 6). The excitation energies were determined from the focal-plane calibration of the spectrometer. The measured differential cross sections are shown in sect. 4, fig. 5. Differential cross sections for elastically scattered deuterons were also measured from $\theta = 10°$ to 48° with the same set-up. This was useful as a check on the deuteron optical potential and for the absolute determination of the differential cross sections by normalizing to optical-model (OM) calculations. The uncertainty due to this normalization is less than 10%. Since no elastic-scattering data of 40–50 MeV ^{3}He on ^{50}Ti were available we also measured the differential cross sections for elastic scattering of ^{3}He from ^{51}V at 43 MeV from $\theta = 8°$ to 50° to obtain a good OM parameter set for the ^{3}He particles. This experiment was performed at the AVF cyclotron of the Vrije Universiteit in Amsterdam. [See ref. [10]) for details about the experimental set-up.]

3. DWBA analysis

In the simple shell-model the 28 neutrons of ^{51}V form a closed shell and the last three of the 23 protons occupy the $1f_{7/2}$ orbit. At low excitation energies in ^{50}Ti levels populated by pick-up from the $1f_{7/2}$, $2s_{1/2}$ and $1d_{3/2}$ orbits should occur. Pick up from the $1d_{5/2}$, $1p_{3/2}$, $1p_{1/2}$ and $1s_{1/2}$ orbits can be found as part of the ^{3}He continuum starting at an excitation energy of about 7 MeV.

In order to deduce spectroscopic information for transitions observed in the ^{51}V(d, ^{3}He)^{50}Ti reaction up to ~7 MeV excitation, DWBA calculations have to be performed to compare with the experimental data. One of the main problems in such a DWBA calculation is the prescription to be used in deriving the form factor for the single particle (s.p.) transfer. It has been argued in the literature [11-15]) that for the pick-up from (stripping to) a non-closed shell target nucleus, the form factors (overlap functions) for s.p. transfer should be obtained from a Hartree-Fock (HF)

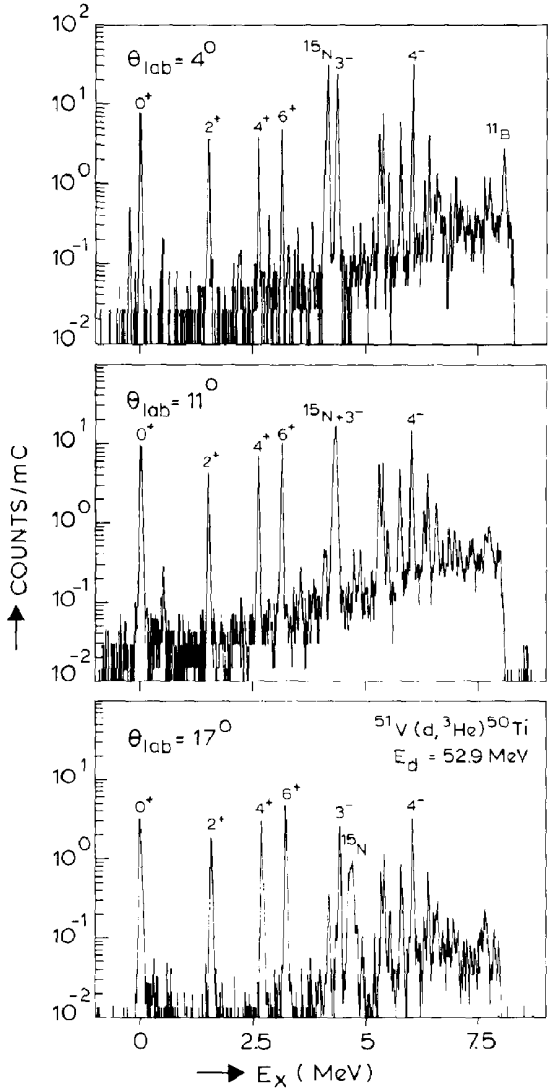

Fig. 2. Spectra taken at 4°, 11° and 17° lab angle. $l = 0$, 3 and 2 particle transfer have distributions which are pronounced at 4°, 11° and 17°, respectively.

calculation in which the set of HF coupled equations have eigenvalues equal to the s.p. separation energies. In this way, the effect of the residual interaction (which is responsible for removing the degeneracy of multiplets of the same configuration but different J) on the radial shape of the overlap functions is properly taken care of. Though this seems to be the correct approach [11-15]) to be used in such a situation, it has to our knowledge never been applied for the actual analysis of any s.p. transfer experiment. It is indeed, as pointed out by Pinkston and Satchler [11]), highly imprac-

tical to perform a Hartree-Fock type calculation even for pure configurations every time a s.p. transfer reaction is performed.

A few guidelines could be followed [11]), however, to ensure that the form factor for s.p. transfer, obtained as a s.p. wavefunction generated in a Saxon-Woods potential well, approximates the overlap function derived from an HF calculation with s.p. separation energies as eigenvalues. First, the single-particle wavefunction should have the correct asymptotic form for large r, where the decay length of the tail of the wavefunction is determined by the separation energy. Second, the Saxon-Woods potential geometry should be modified for the different final states populated by the same j-transfer to reflect the effects of the residual interaction. Because for final states with the same configuration but different spin J, it is the non-scalar components in the multipole expansion of the residual interaction which lead to the removal of the degeneracy of the multiplet and since furthermore these non-scalar components must vanish at the center of the nucleus, Pinkston and Satchler [11]) concluded that the contribution to the effective potential will peak at the surface. In our case, ^{51}V(d, ^{3}He)^{50}Ti reaction, the 0^+, 2^+, 4^+ and 6^+ quadruplet final states in ^{50}Ti reached by the reaction have excitation energies that increase with spin. Hence the binding energy of the removed proton increases with the spin of the final state of the quadruplet and therefore the effect of the residual interaction is to increase the effective binding potential of the removed "third" proton. If following Pinkston and Satchler [11]) the depth of the potential in the nuclear interior does not change, then we expect that the radius of the potential well of the removed single particle should increase as a function of the spin J for states of the quadruplet populated by the reaction and belonging to the same final configuration. In our DWBA analysis we will be guided by these general considerations as well as by the results of a recent (e, e'p) experiment for the spectroscopic factors to the transitions to the ground state multiplet in ^{50}Ti. The (e, e'p) results do not suffer from the selectivity of the (d, ^{3}He) reaction which is mainly sensitive to the nuclear surface region.

Before establishing the DWBA procedure to be used in our final analysis we consider first the usual uncertainties in the DWBA calculations due to variations of various parameters and/or use of different corrections.

DWBA calculations with the code DWUCK4 [16]) were performed to describe the measured (d, ^{3}He) differential cross sections. The incoming deuteron and outgoing ^{3}He distorted waves were generated from OM potentials, which were determined by fitting the measured elastic cross sections. The OM potential has the usual form:

$$U_{\mathrm{opt}}(r) = -V_0 f(r, r_0, a_0) - iW_{\mathrm{v}} f(r, r_i, a_i) + 4ia_i W_{\mathrm{d}} f'(r, r_i, a_i) + 2V_{ls}\boldsymbol{l}\cdot\boldsymbol{s}\frac{1}{r}f'(r, r_{ls}, a_{ls}) + V_{\mathrm{C}}(r, r_{\mathrm{C}}),$$

where V_0, W_{v}, W_{d} and V_{ls} are the depths of the real, imaginary volume and surface, and spin-orbit potentials. V_{C} is the Coulomb potential. $f(r, r_0, a_0)$ is the usual

Saxon-Woods form and $f'(r, r_i, a_i)$ its derivative. The OM parameters for the deuterons are listed in table 1. Sets 1 and 2 were obtained from a fit to the measured elastic cross sections. In set 1 the radius of the potential is chosen to a value frequently used in elastic deuteron-scattering analyses [2]). In set 2 this radius is fixed to the value used in an adiabatic potential [17]). Set 3 is a folded Becchetti-Greenlees potential [18]), which was not fitted to the data, but was used to see the effect of using an adiabatic potential in the DWBA calculations.

We found five OM parameter sets describing the elastic ^{3}He scattering from ^{51}V. They are summarized in table 2. The sets differ in the use of surface or volume absorption and shallow or deep real potential, or in the real radius.

Differential cross sections for $l=0$, $l=2$ and $l=3$ transfer at 4 MeV excitation energy were calculated. Only the ^{3}He set 3 together with the deuteron sets 1, 2 and 3 and the ^{3}He set 5 together with the deuteron sets 1 and 2 were able to reproduce the measured shapes of the angular distributions. The shallow ^{3}He OM parameter sets gave bad fits to the data and were rejected. We have compared the magnitude of the DWBA cross sections using these five combinations of potentials. As a standard we have chosen ^{3}He set 3 together with deuteron set 2. The cross sections calculated using the other combinations, relative to the one calculated with the standard set, are summarized in table 3. We conclude that there is a 5% uncertainty in the deduced spectroscopic factors due to the choice of different deuteron OM parameter sets obtained by fitting the measured elastic data, while using the folded

TABLE 1

Optical-model parameters for ^{51}V + 52.9 MeV deuterons
(depths are in MeV and lengths are in fm)

set	V_0	r_0	a_0	W_d	W_v	r_i	a_i	V_{ls}	r_{ls}	a_{ls}
1	92.52	1.05	0.925	13.81		1.319	0.757	4.31	1.01	0.40
2	81.48	1.17	0.823	14.07		1.266	0.782	4.09	1.01	0.40
3	95.65	1.17	0.779	11.48	6.35	1.290	0.611	6.20	1.01	0.75

$r_C = 1.30$ fm for all 3 sets.

TABLE 2

Optical-model parameters for ^{51}V + 42.8 MeV ^{3}He
(depths are in MeV and lengths are in fm)

set	V_0	r_0	a_0	W_d	W_v	r_i	a_i	V_{ls}	r_{ls}	a_{ls}
1	117.1	1.215	0.722	20.55		1.244	0.803	2.60	1.05	0.20
2	127.8	1.140	0.778	21.10		1.277	0.770	2.60	1.05	0.20
3	168.6	1.185	0.681	22.65		1.166	0.860	2.60	1.05	0.20
4	135.9	1.090	0.788		12.55	1.736	0.728	2.60	1.05	0.20
5	186.5	1.100	0.728		15.00	1.657	0.783	2.60	1.05	0.20

$r_C = 1.30$ fm for all 5 sets.

TABLE 3

Calculated relative cross sections for different combinations of optical-model potentials

potential set ^{3}He	d	$l=0$	$l=2$	$l=3$
3	1	0.98	0.98	0.95
3	2	1.00	1.00	1.00
3	3	1.25	1.15	1.15
5	1	1.03	1.01	1.13
5	2	1.06	1.06	1.20

Becchetti-Greenlees OM parameter set leads to differences as large as 20%. The uncertainty due to the choice of a ^{3}He optical-model parameter set is small for $l=0$ and $l=2$ ($\approx$5%), but large for $l=3$ ($\approx$20%) as can be seen from table 3.

Non-locality and finite-range effects in the local energy approximation (LEA) were also investigated using the standard OM parameter sets 3 and 2 for the ^{3}He and the deuteron, respectively. The non-locality corrections on the OM wavefunctions have small effects on the magnitude (see table 4) and the shape of the calculated cross sections. If we take finite-range effects into account, the calculated cross sections are 10-60% larger. Here the shape changes as well; the cross section at forward angles increases and at backward angles increases less ($l=0$, $l=3$) or even decreases ($l=2$), yielding a better description of the measured data.

Finally the sensitivity of the calculated cross sections to various parameters related to the BSWF, such as the radius and diffuseness of the binding potential and the binding energy of the transferred particle, were investigated along with the sensitivity due to non-locality in the BSWF. In general the form of the calculated differential cross section did not change much; only its magnitude changed. The effects on the magnitude are summarized in table 4. Note that the changes do not have the same effect on transitions with different l-values. The rms radii corresponding to the different BSWF's are also listed in table 4. There is a correlation between the rms radius and the relative change in cross section as can be seen from fig. 3. A change of 1% in the rms radius of the BSWF will change the spectroscopic factor by about 10%, therefore one has to know the rms radius of the BSWF very accurately to obtain reliable spectroscopic factors. This effect has also been reported earlier [see refs. [6,19]) and references therein]. However, the rms radius is not the only determining factor as the points in fig. 3 do not lie on a smooth curve.

In order to investigate which part of the BSWF gives the largest contribution to the DWBA cross section, cross sections were calculated for $l=0$, $l=2$ and $l=3$ transfer with different lower radial cutoffs. The results are shown in fig. 4 together with the used BSWF. One sees clearly that the main contribution to the cross section, especially in the first maximum from which C^2S is usually determined, comes from the region from 6.0 to 8.0 fm, which is outside the nucleus and in the exponential

TABLE 4

Changes in the calculated cross section, when one parameter changes [a])

Parameter	$l=0$ (%)	r_{rms} (fm)	$l=2$ (%)	r_{rms} (fm)	$l=3$ (%)	r_{rms} (fm)
d and ^{3}He not local	+2		+3		+3	
Finite range corr.	+60		+18		+10	
$r_0=1.215$		3.60		3.54		3.89
$r_0=1.200$	−7	3.57	−8	3.51	−9	3.86
$r_0=1.255$	+21	3.66	+24	3.63	+25	3.99
$a_0=0.65$	−11	3.55	−12	3.52	−11	3.87
$E_b=-13.057$	−17	3.56	−16	3.51	−14	3.87
$E_b=-11.057$	+22	3.63	+21	3.57	+15	3.92
BSWF not local	+16	3.68	+16	3.59	+20	3.95

[a]) Changes are given in percentages relative to a standard calculation which uses the following parameters: BSWF: $r_0=1.215$ fm, $a_0=0.70$ fm. Binding energy: 12.057 MeV ($E_x=4.0$ MeV). Local zero range. Parameter set 3 for ^{3}He and parameter set 2 for d.

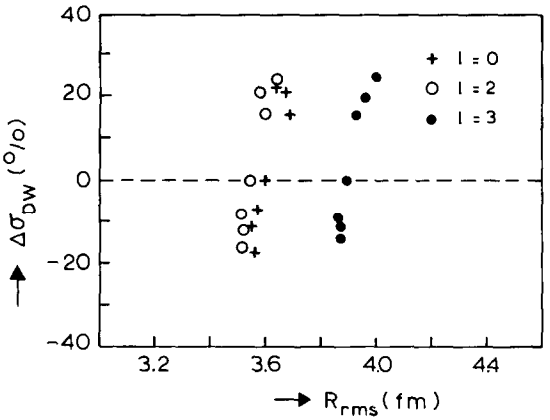

Fig. 3. Percentage changes in DWBA cross sections versus the rms radius.

tail of the BSWF. This confirms the known fact that the (d, ^{3}He) reaction only measures the asymptotic normalization of the BSWF.

It can be concluded from the above that the spectroscopic factors obtained from the analysis of the (d, ^{3}He) reaction are very sensitive to the choice of the parameters used in the calculations. Consequently there is a great uncertainty in the spectroscopic factors obtained from the analysis of the (d, ^{3}He) reaction.

There is the additional uncertainty which is related to how one treats levels populated by the same l transfer at different excitation energies, i.e., different binding energies. It has been pointed out earlier that the best method is to obtain the overlap functions from a HF calculation. However, the BSWF is usually obtained using the so-called separation-energy method. Since the geometry of the well is kept constant, one could call it the fixed geometry method. This involves solving a Schrödinger

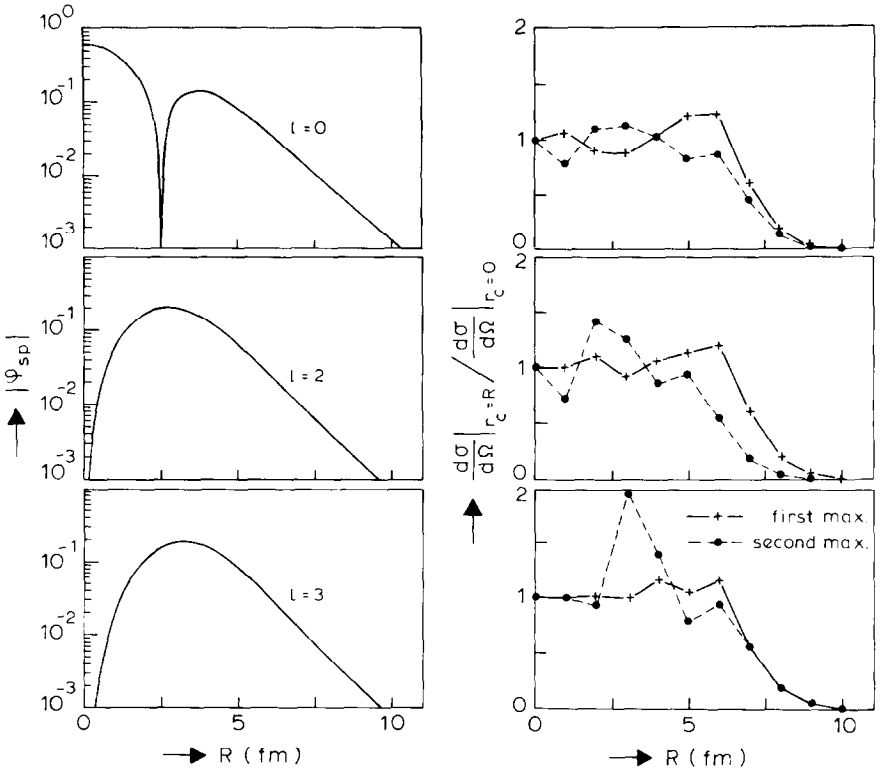

Fig. 4. Integrated part of the cross section versus the lower cutoff radius for $l = 0$, $l = 2$ and $l = 3$ transfer. The solid and dash-dotted curves refer to the first and second maxima in the predicted DWBA cross sections. The curves in the left section of the figure show the respective bound-state wavefunctions.

equation for a proton bound in a Saxon-Woods potential well, the depth of which is adjusted to reproduce the separation energy of the proton. As a result the rms radius of the calculated BSWF decreases rapidly with increasing excitation (binding) energy. This is clearly not a correct procedure as discussed by various authors [11-15]). Another option would be to change the geometry in such a way as to keep the rms radius constant, since there is no obvious *a priori* reason for changing the rms radius of the $1f_{7/2}$ orbit if the final nucleus is left in an excited state. This in fact leads to a change in the radius of the effective binding Saxon-Woods potential in accordance with the criteria of Pinkston and Satchler [11]).

In order to study the difference between both methods we have performed calculations with both methods to generate the BSWF. In the first method (the usual separation-energy method) a Saxon-Woods potential with radius parameter 1.256 fm and diffuseness 0.70 fm was used. These values were obtained by fixing the rms radius of the BSWF for the transition to the ground state to 4.10 fm, a value given by magnetic electron scattering data [20]). The value of 4.10 fm was obtained from the value given in ref. [20]), table XV, by transforming it to the proton-(A-1) system,

as is needed in pick-up calculations. We shall refer to this as method 1. In the second method, which could be called the rms method, the rms radius for the $1f_{7/2}$ orbit was kept fixed to 4.10 fm, whereas the potential radius and the well depth were adjusted to reproduce this rms value. The problem of this method, is that electron scattering data give only the rms radius of the $1f_{7/2}$ orbit; the $2s_{1/2}$ and the $1d_{3/2}$ rms radii cannot be determined in this way. The spectroscopic factors obtained using both methods are described in the next section.

4. Spectroscopic results and discussion

In fig. 5 we show the measured differential cross sections together with the results of non-local, finite-range (in the local energy approximation) DWBA calculations. In general the measured angular distributions are well described by the DWBA calculations.

The spectroscopic factors were determined using the relation [21])

$$\left.\frac{d\sigma}{d\Omega}\right|_{exp} = \frac{2.95 C^2 S}{2j+1} \left.\frac{d\sigma}{d\Omega}\right|_{DW}$$

assuming one l transfer.

We first discuss the results for the low-lying quadruplet of states in ^{50}Ti populated by $1f_{7/2}$ proton pick-up. The spectroscopic factors obtained using both methods for the $1f_{7/2}$ pick-up to the ground state quadruplet are given in table 5. These are compared with the values from literature obtained from the (d, ^{3}He) data using similar prescriptions. Comparing our results obtained with method 1 (column 3) to those of Craig *et al.* [5]) (column 4) obtained using the same energy separation method with a fixed geometry for the binding Saxon-Woods potential and applying finite range and non-locality corrections (also for the BSWF) we find excellent agreement. If we use method 2 the spectroscopic factors are modified in such a way that for higher values of J the spectroscopic factors become relatively smaller. Comparing our results obtained using method 2 (column 6) to those of Moalem and Vardi [6]) (column 5) obtained using a similar method with a constant rms radius for the $1f_{7/2}$ orbit of 3.99 fm but neglecting non-locality corrections for the BSWF, we observe that our values are much smaller as expected from increasing the rms radius and including the BSWF non-locality corrections. Interestingly enough, however, the relative spectroscopic factor values listed within the square brackets are in rather good agreement.

In table 5, column 7, we also list the spectroscopic factors obtained from the ^{51}V(e, e'p) reaction [1]). These are rather insensitive to the details of the BSWF used in the analysis. In strong contrast to earlier results from the (d, ^{3}He) data, in which the DWBA analysis was performed [2,3]) in zero range without non-locality corrections yielding spectroscopic factors in agreement with a pure $(1f_{7/2})^3$ configuration for

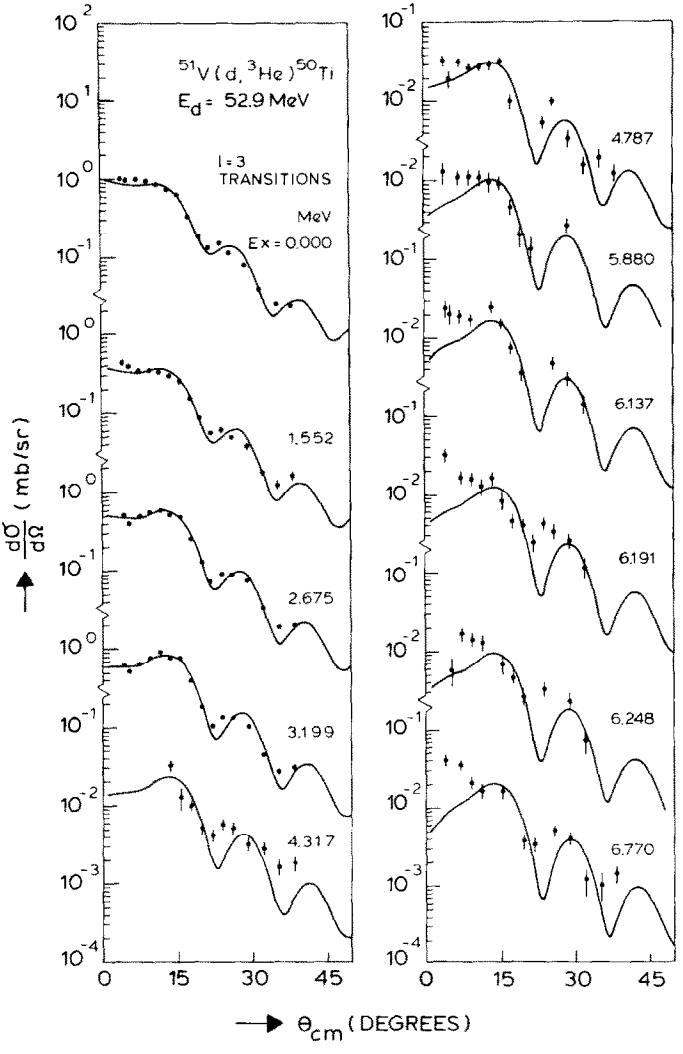

Fig. 5a

Fig. 5. Measured cross sections together with the results of non-local finite-range DWBA calculations.

the ground state of ^{51}V, the (e, e'p) results indicate a strong depletion of the $1f_{7/2}$ spectroscopic strength as compared with the simple shell-model predictions. They are even 40% to 50% smaller as compared with our values and those of Craig *et al.* [5]). If taken at their face value these results for the absolute spectroscopic factors clearly show the fallacy in the common practice of adjusting parameters employed in the DWBA analysis in such a way as to exhaust the spectroscopic strength sum rule near closed shells. Also the value for the radius of the proton $1f_{7/2}$ orbit

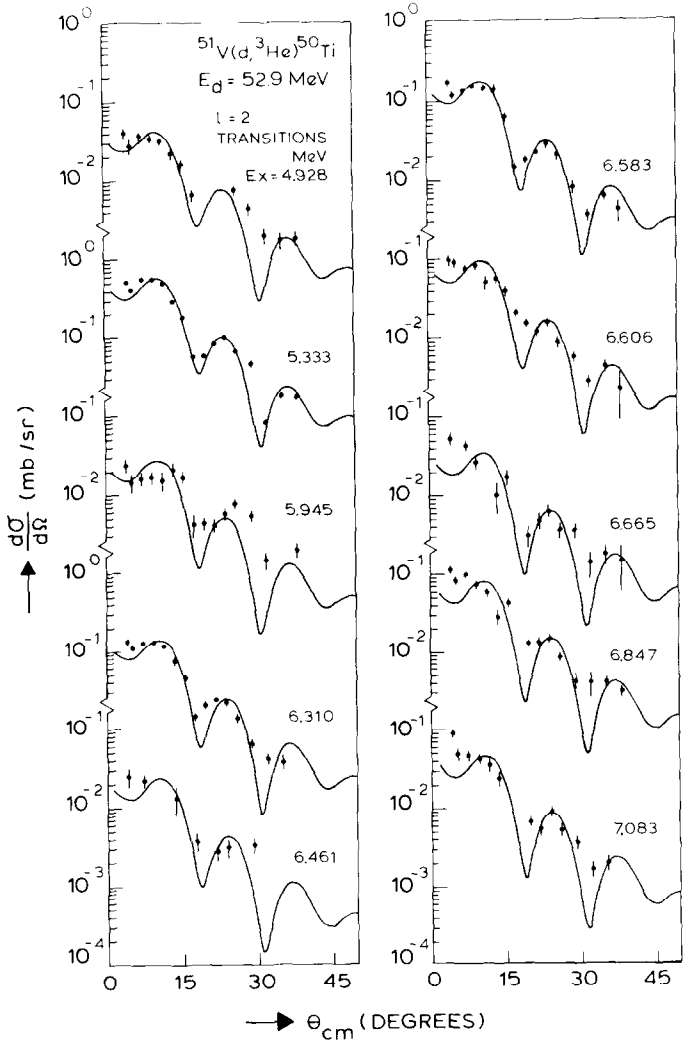

Fig. 5b

obtained [6]) from the results of stripping and pick-up reactions with the help of spin-dependent sum rule [22]) would be too small because that analysis finds a summed spectroscopic strength for the low-lying states of about 3.0.

The results listed in table 5 indicate a preference for the rms method. This is based on the fact that the relative spectroscopic factors, for the states with the larger absolute spectroscopic factors (i.e. 0^+, 4^+ and 6^+), determined using the rms method are irrespective of the assumed rms radius value in better agreement with the values determined from the (e, e'p) reaction, which are rather insensitive to the details of the BSWF. Furthermore, the radius of the binding Saxon-Woods potential needed

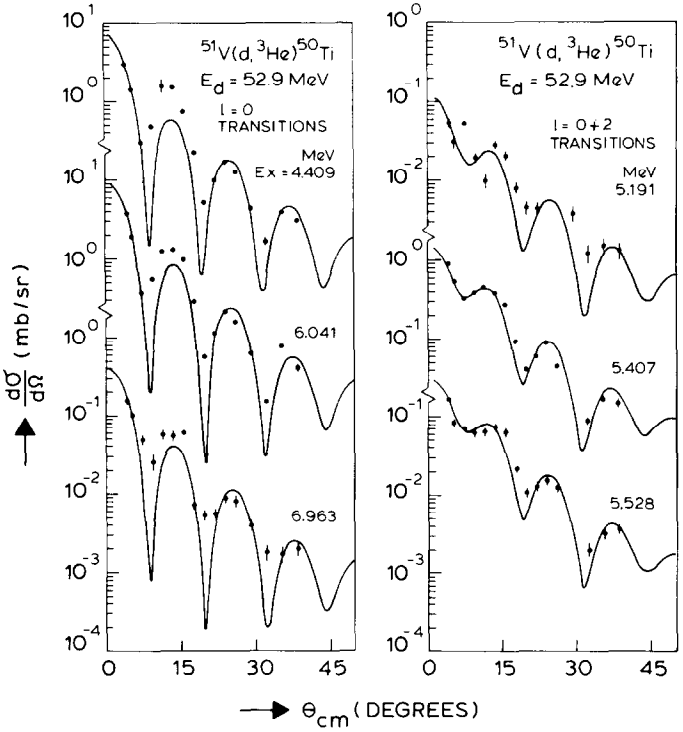
$^{51}V(d,{}^3He)^{50}Ti$
E_d = 52.9 MeV
l = 0
TRANSITIONS
MeV
Ex = 4.409
6.041
6.963
l = 0+2
TRANSITIONS
MeV
5.191
5.407
5.528
$\frac{d\sigma}{d\Omega}$ (mb/sr)
θ_{cm} (DEGREES)

Fig. 5c

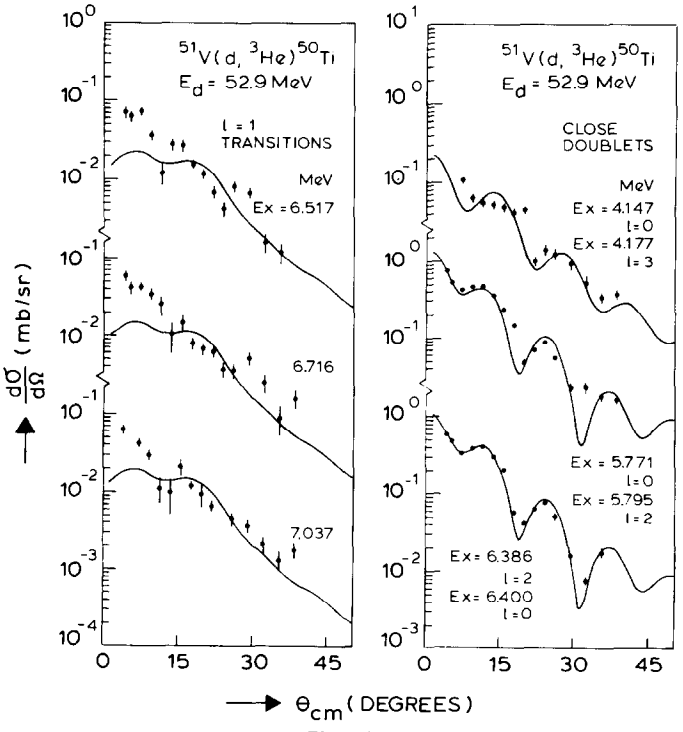
$^{51}V(d,{}^3He)^{50}Ti$
E_d = 52.9 MeV
l = 1
TRANSITIONS
MeV
Ex = 6.517
6.716
7.037
CLOSE
DOUBLETS
MeV
Ex = 4.147
l = 0
Ex = 4.177
l = 3
Ex = 5.771
l = 0
Ex = 5.795
l = 2
Ex = 6.386
l = 2
Ex = 6.400
l = 0
$\frac{d\sigma}{d\Omega}$ (mb/sr)
θ_{cm} (DEGREES)

Fig. 5d

TABLE 5

Spectroscopic factors of the $1f_{7/2}$ proton pick-up strength of the quadruplet of states in ^{50}Ti obtained from the present ^{51}V(d, ^{3}He) results using different prescriptions [a]) for the BSWF in the DWBA analysis in comparison to values from the literature. (Spectroscopic factor values relative to that of the 0^+ ground state are given in square brackets)

E_x (MeV)	J^π	C^2S [b]) present work method 1	C^2S [b]) ref. [5]) method 1	C^2S [c]) ref. [6]) method 2	C^2S [d]) present work method 2	C^2S [e]) ref. [1])	C^{Sf}) present work method 2	Theory ref. [23])
0.000	0^+	0.41 [1.00]	0.41 [1.00]	0.64 [1.00]	0.41 [1.00]	0.30 [1.00]	0.30 [1.00]	0.75 [1.00]
1.552	2^+	0.22 [0.54]	0.23 [0.56]	0.31 [0.48]	0.20 [0.49]	0.13 [0.43]	0.15 [0.50]	0.42 [0.56]
2.675	4^+	0.41 [1.00]	0.42 [1.02]	0.57 [0.89]	0.35 [0.85]	0.27 [0.90]	0.26 [0.87]	0.75 [1.00]
3.199	6^+	0.65 [1.59]	0.73 [1.78]	0.92 [1.43]	0.53 [1.29]	0.41 [1.37]	0.39 [1.30]	1.08 [1.44]
$\sum C^2S$		1.69	1.79	2.44	1.49	1.11	1.10	3.00

[a]) Method 1 is the usual separation energy method; in method 2 the rms radius is kept constant.
[b]) DWBA analysis using finite range and non-local (FRNL) corrections also for BSWF.
[c]) $1f_{7/2}$ orbit rms radius taken to be 3.99 fm.
[d]) $1f_{7/2}$ orbit rms radius taken to be 4.10 fm.
[e]) From (e, e'p); $1f_{7/2}$ orbit rms radius = 4.20 fm.
[f]) $1f_{7/2}$ orbit rms radius taken to be 4.20 fm.

to keep the $1f_{7/2}$ orbit rms radius constant increases as expected from the theoretical considerations as outlined (see sect. 3) by the arguments of Pinkston and Satchler [11]). For a rms radius of 4.10 fm for the $1f_{7/2}$ orbit, the radius of the binding potential increases from 1.256 fm for the $J^\pi = 0^+$ to 1.297 fm for the $J^\pi = 6^+$.

Two further remarks can be made concerning the spectroscopic factors listed in table 5. The spectroscopic factors we obtain from our (d, ^{3}He) analysis are based on a rms radius of the $1f_{7/2}$ orbit of 4.10 fm. The rms radius deduced from the (e, e'p) study [1]) for the $1f_{7/2}$ transitions to all states of the $(1f_{7/2})^2$ quadruplet in ^{50}Ti is 4.20 (14) fm. If instead we fix the $1f_{7/2}$ rms orbit radius to this value in our calculations we obtain the spectroscopic factors listed in column 8 of table 5, which are in excellent agreement with those deduced from the (e, e'p) reaction. The second interesting remark to be made is that although both the (e, e'p) and our results indicate strong depletion of the $1f_{7/2}$ strength compared with the predictions of the simple shell model [23]) (listed in the last column), there is surprising agreement between the relative spectroscopic values deduced from all available experiments and those predicted by the simple shell model [23]). This indicates that if depletion is due to removing of spectroscopic strength to higher excitation energies, it occurs proportionately for all J^π values.

In the literature a number of shell model calculations on ^{51}V have been reported, differing in the model Hilbert space used for the calculations and also in the residual nucleon-nucleon interaction used. The earliest of these calculations was by Lips and McEllistrem [24]) which included in addition to the major $(1f_{7/2})^3$ proton configuration, configurations of the type $(1f_{7/2})^2 2p_{3/2}$ and also $(1f_{7/2})^2 1f_{5/2}$ and used an

adjusted surface delta interaction. The results for the $1f_{7/2}$ spectroscopic factors for the ground state quadruplet do not differ appreciably from those predicted by the simple shell model except for the 2^+ state, where part of the $1f_{7/2}$ strength ($\sim$15%) is removed to a 2^+ state at higher energy ($E_x = 3.36$ MeV). Similar results were quoted by Craig *et al.* [5]) from unpublished work by Van der Merwe [25]) in which excitations to the $1f_{5/2}$ orbit were not allowed, but instead excitations of $1f_{7/2}(2p_{3/2})^2$ type were taken into consideration. In a more sophisticated calculation Rustgi *et al.* [26]), employing a ^{48}Ca core and Kuo-Brown [27]) matrix elements for the residual interaction, allowed all possible 1f-2p configurations in their shell-model calculations. Also here the ^{51}V ground state was found to be $\sim$92% of the $(1f_{7/2})^3$ configuration. More recently Sandhu and Rustgi [28]) used the Kuo-Brown matrix elements in a Hartree-Fock-Bogoliubov calculation in which ^{40}Ca was assumed to be a closed core. The 3 protons and 8 neutrons were allowed to occupy the $1f_{7/2}$, $1f_{5/2}$, $2p_{3/2}$ and $2p_{1/2}$ orbitals. Surprisingly enough, the pick-up strength for the $1f_{7/2}$ protons was reduced to 2, whereas the proton pick-up strengths for the $1f_{5/2}$, $2p_{3/2}$ and $2p_{1/2}$ were found to be 0.12, 0.75 and 0.13, respectively. Whereas the summed $1f_{7/2}$ proton pick-up spectroscopic strength is in reasonable agreement with our experimental results (see also tables 7 and 8), the $2p_{3/2}$ strength to the low-lying states in ^{50}Ti as obtained from our experiment is almost negligible, in apparent contradiction to the results of Sandhu and Rustgi [28]).

To investigate this problem further, we have performed extensive shell-model calculations for both positive- and negative-parity states of ^{50}Ti. The wavefunctions have been obtained in a model space that includes particle-hole excitations of protons as well as neutrons with respect to the simple shell-model description of ^{51}V and ^{50}Ti i.e., $\pi(f_{7/2})^3\nu(f_{7/2})^8$ and $\pi(f_{7/2})^2\nu(f_{7/2})^8$, respectively. It turns out that the neutron particle-hole excitations with respect to the $N = 28$ core cannot be ignored. In fact we find that for the wavefunctions of ^{51}V and ^{50}Ti the total intensity of the components with neutron p-h excitations is often considerably larger than that with proton p-h excitations.

The model space employed for the calculation of spectroscopic factors for the positive-parity states of ^{50}Ti has been restricted to the four fp-shell orbits. The total number of particle-hole excitations (protons and/or neutrons) has to be limited to two, since this already leads to hamiltonian matrices with orders up to about 1400. The interaction used is similar to the one described in ref. [29]), except that the empirical modification of the Kuo-Brown matrix elements [27]) has been obtained from a fit to levels in the $A = 42$–58 nuclei [30]). Following the same procedure as in ref. [31]) a scaling factor of 0.75 had to be applied to the hamiltonian matrix elements.

The results for the low-lying quadruplet are given in table 6 together with the spectroscopic factors obtained from the simple $\pi(f_{7/2})^n$ description of ^{51}V and ^{50}Ti. It follows that the excitation energies of the yrast $J^\pi = 0^+$, 2^+, 4^+ and 6^+ states in ^{50}Ti are well reproduced. The admixtures of particle-hole components in ^{51}V and ^{50}Ti are about 30% in intensity, but reduce the spectroscopic factors by only 5–20%

TABLE 6
Shell-model results

J^π	E_x (MeV)		C^2S	
	exp.	calc.	$f_{7/2}^n$	present calc.
0^+	0	0	0.75	0.72
2^+	1.55	1.65	0.42	0.34
4^+	2.68	2.72	0.75	0.64
6^+	3.20	3.06	1.08	0.95

as follows from table 6. In order to apply the sum rule for $l=3$ transfer the calculated proton occupation numbers for the ground state of ^{51}V are of interest. For the various subshells these are given by $\langle f_{7/2}\rangle = 2.84$, $\langle f_{5/2}\rangle = 0.11$, $\langle p_{3/2}\rangle = 0.04$ and $\langle p_{1/2}\rangle = 0.01$. Hence it follows from the present calculations that the $J^\pi = 0^+$, 2^+, 4^+ and 6^+ yrast states contain 93% ($\sum C^2S = 2.65$, see table 6) of the total $1f_{7/2}$ pick-up strength ($\sum C^2S = 2.84$). The remaining part of the calculated strength is distributed over many weakly excited higher-lying states, consistent with the experimental results.

The negative-parity states of ^{50}Ti have been described in a model space in which the coupling of one $s_{1/2}$ or $d_{3/2}$ hole to the wavefunctions of the ground state and excited states in ^{51}V is taken into account. The latter wavefunctions have been obtained in a 1p-1h model space with respect to the $\pi(f_{7/2})^3\nu(f_{7/2})^8$ configurations with the particle-hole pair consisting of either protons or neutrons. The largest dimension is reached for the 4^- state in ^{50}Ti with about 450 components.

Since the model space used for the $l=0$ and $l=2$ transfer differs from that for the calculation of $l=3$ transfer one cannot use the same effective interaction as has been obtained for the positive-parity states. Hence, we choose the Surface Delta Interaction (SDI) with the $T=0$ and $T=1$ strength parameters given by (25/A) MeV as suggested in ref. [23]). The single-particle energies for the fp-shell orbits have been taken as the averaged values from the work of Yokoyama and Horie [33]). The only free parameter that remains to be fixed is the energy gap Δ(s-d) between the $s_{1/2}$ and $d_{3/2}$ effective single-particle energies. The value Δ(s-d) = 1.0 MeV, with the $s_{1/2}$ orbit above the $d_{3/2}$, reproduces quite well the observed splitting between $l=0$ and $l=2$ spectroscopic factors in ^{50}Ti (see below). Admixtures of components containing 1p-1h excitations with respect to the dominant $(sd)^{-1}(f_{7/2})^n$ components of ^{50}Ti are found to be strong (about 40%). The results of this calculation will be discussed below (see also fig. 6).

In comparing calculated spectroscopic factors with measured ones for these negative-parity states there is a difficulty. It has been argued above that the rms method (method 2) is preferable to the fixed geometry of the binding potential method (method 1). However, this method is difficult to apply for more deeply-bound states, such as the $2s_{1/2}$ and $1d_{3/2}$ states in ^{51}V, because the rms radii of these orbits

are not known. The following procedure was used to estimate the rms radii of these orbits. For the $2s_{1/2}$ orbit we have estimated the rms radius to be 3.71 fm by taking the average of the $2s_{1/2}$ rms radii determined at 4.4 MeV and 6.05 MeV excitation energy where two strong $l=0$ transitions are observed, employing the potentials used to calculate the $1f_{7/2}$ BSWF at these excitation energies. A similar calculation was also performed for the $1d_{3/2}$ orbit resulting in a rms radius of 3.73 fm.

The calculated and observed spectroscopic factors for $l=0$ and $l=2$ are compared in fig. 6 as a function of excitation energy. The observed distribution of spectroscopic factors for $l=0$ and $l=2$ transfer is quite well reproduced by the present calculations, in particular the occurrence of only two strong $l=0$ peaks in the $E_x=4$–7 MeV

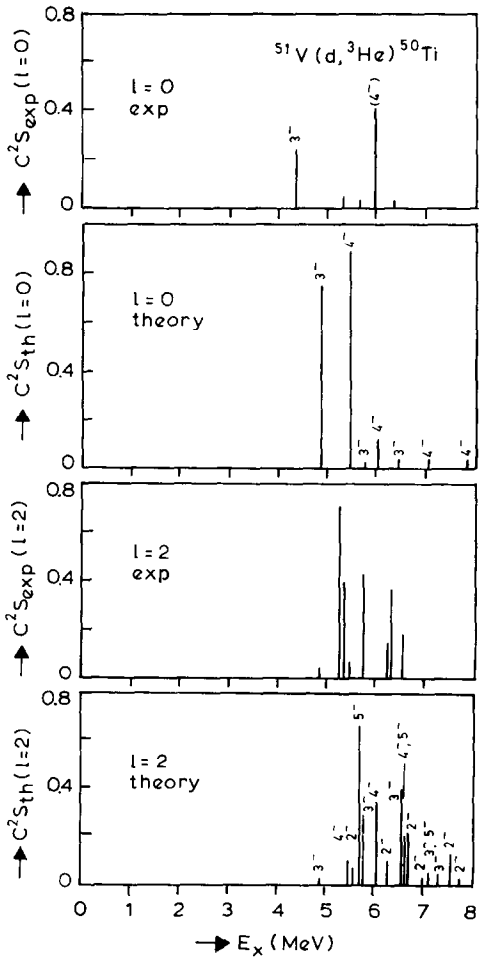

Fig. 6. Theoretical and experimental spectroscopic strength distributions for $l=0$ and $l=2$ proton pick-up from ^{51}V.

region and of several rather strong $l=2$ peaks in the $E_x = 5$–7 MeV region. Theoretically about 90% of the total $l=0$ and $l=2$ strength is concentrated below $E_x = 8$ MeV, i.e., $\sum C^2S(l=0) = 1.87$ and $\sum C^2S(l=2) = 3.56$, respectively.

Because the $l \cdot s$ splitting between the $d_{3/2}$ and $d_{5/2}$ orbits is several MeV, we do not expect a significant part of the $d_{5/2}$ hole strength below $E_x = 8$ MeV. However, a more quantitative description cannot be given, because the inclusion of $d_{5/2}$ hole states in the ^{50}Ti wavefunctions would lead to shell-model calculations which are presently still unfeasible.

In table 7 we list the spectroscopic factors for all other transitions observed in this experiment up to an excitation energy of about 7 MeV, using both methods described in the previous section, and compare them with spectroscopic factors obtained from previous experimental work [2,3]). If we compare the absolute spectroscopic factors, the spectroscopic factors obtained in this experiment are much smaller than the ones obtained earlier, although the measured cross sections agree with the ones of ref. [2]). This can be explained as has already been discussed earlier by the fact that we have used a non-local finite-range calculation, whereas the earlier experiments of refs. [2,3]) were analysed using local zero-range, and with a different BSWF.

In table 8 the summed strengths of the $l=0$, $l=2$ and $l=3$ transitions found in various experiments is given. Most of the strength for $l=3$ transitions is exhausted by the ground state quadruplet. There were no indications of $l=1$ admixtures in the 2^+ and 4^+ states ($C^2S < 0.01$). Taking into account all $l=3$ transitions up to 7 MeV excitation energy and keeping the radius of the potential fixed to 1.256 fm (method 1), the sum of the spectroscopic factors is 1.89. This is less than expected from the simple shell-model picture and from the more extensive shell-model calculation. If we keep the rms radius of the $1f_{7/2}$ orbit fixed to 4.10 fm (method 2) the sum becomes 1.63. This is about two thirds of the value expected from the extensive shell-model calculation.

For the $l=0$ transitions there are two strong peaks, which contain most of the strength: the 3^- level at 4.409 MeV and the 4^- level at 6.041 MeV (see table 7). The total sum using method 1 is 0.87, which is less than half the expected value from the extensive shell-model calculation. We have only analysed states up to 7 MeV excitation energy. However, we observed in the spectra taken at very forward angles two $l=0$ transitions to states at 7.605 and 7.697 MeV, which could add 0.1 proton to the $l=0$ strength. Using method 2 the sum is 0.72 where we have taken 3.71 fm as rms radius of the orbit for the $2s_{1/2}$ protons. As mentioned earlier there are yet no measurements of the rms radius of the $2s_{1/2}$ orbit.

Simple shell theory predicts for the $l=2$ transfer four states, i.e., 2^-, 3^-, 4^-, and 5^- states. In the present experiment we observed six strong $l=2$ transitions containing about 85% of the observed $l=2$ strength. The state at 5.795 MeV is mentioned [31]) as a $(4, 5)^-$ state, whereas for the other states no spin and parity assignments are known. The remaining part of the $l=2$ strength is fragmented into a large number

TABLE 7

Levels observed in this experiment together with determined spectroscopic factors in comparison with values known from the literature

E_x [a]) (MeV)	l	C^2S method 1	C^2S method 2	C^2S ref. [2])	C^2S ref. [3])	E_x ref. [32])	J^π
0.000	3	0.41	0.41	0.73	0.74	0.000	0^+
1.552	3	0.22	0.20	0.39	0.37	1.554	2^+
2.675	3	0.41	0.35	0.64	0.75	2.675	4^+
3.199	3	0.65	0.53	1.05	1.14	3.199	6^+
4.147	0	0.008	0.008			4.147	4^-
4.177	3	0.047	0.035			4.172	$(3,4)^+$
4.317	3	0.022	0.016			4.311	2^+
4.409	0	0.26	0.22	0.63	0.77	4.411	3^-
4.787	3	0.042	0.024			4.789	
4.928	2	0.051	0.027				
5.191	0+2					5.186	
	0	0.006	0.006				
	2	0.019	0.019				
5.333	2	0.71	0.35	1.90	1.67	5.346	
5.407	0+2					5.440	
	0	0.064	0.066				
	2	0.40	0.40		0.82		
5.528	0+2						
	0	0.013	0.012				
	2	0.069	0.067				
5.771	0	0.046	0.045				
5.795	2	0.43	0.43			5.807	$(4,5)^-$
5.880	3	0.013	0.009			5.890	
5.945	2	0.028	0.018			5.945	
6.041	0	0.42	0.30	1.10	1.03	6.045	(4^-)
6.137	3	0.021	0.014			6.135	7^+
6.191	3	0.016	0.011				
6.248	3	0.013	0.009			6.250	
6.310	2	0.14	0.092			6.325	
6.386	2	0.36	0.36			6.379	
6.400	0	0.035	0.037			6.440	
6.461	2	0.023	0.014			6.481	
6.517	1	0.009				6.520	
6.583	2	0.18	0.12	1.40	(1.23)	6.592	
6.606	2	0.073	0.061				
6.665	2	0.027	0.023			6.697	
6.716	1	0.006				6.710	
6.770	3	0.023	0.018			6.770	9^+
6.847	2	0.067	0.056				
6.963	0	0.017	0.015				
7.037	1	0.007				7.045	
7.083	2	0.038	0.032			7.092	3^-
	2			1.10	(0.97)	7.65	

[a]) The errors in the excitation energies range from 2 keV at 0 MeV to 10 keV at 7 MeV.

TABLE 8

Summed $l=0$, $l=2$ and $l=3$ strength found in various experiments below $E_x = 7$ MeV

l	Present results		Ref. [2])	Ref. [3])	Theory	
	method 1	method 2			[a])	[b])
0	0.87	0.72	1.73	1.80	2.0	1.87
2	2.62	2.06	4.40	4.69	4.0	3.56
3	1.89	1.63	2.81	3.00	3.0	2.84

[a]) Simple shell model.
[b]) Present extensive shell-model calculation.

of states. Using method 1 we find 74% of the $d_{3/2}$ pick-up strength expected from the extensive shell-model calculation. Here in addition to the uncertainty in the rms radius, uncertainty due to pick-up of protons from the $1d_{5/2}$ shell arises. Method 2 gives 58% of this expected $1d_{3/2}$ pick-up strength. Hinterberger *et al.* [2]) have reported a state at 7.65 MeV, containing 25% of the $l=2$ strength. With our improved resolution, we found a large number of small peaks forming a bump at 7.5 MeV in our spectra. Due to the complexity of this structure no further analysis was attempted. If we assume the measured cross section to be completely due to $l=2$, it would give a spectroscopic factor of about 0.50.

In the present analysis we found three possible candidates for $l=1$ transitions, at 6.517, 6.716 and 7.037 MeV. They are also shown in fig. 5. Spectroscopic factors for these levels are listed in table 7. Only method 1 was used. No further analysis was performed in this case, but the observation of these states indicates that there is some 2p admixture in the ^{51}V ground state.

If one wants to draw conclusions from the comparison of the measured spectroscopic strength with the sum rule or with the results of the extensive shell-model calculation, one must keep in mind the uncertainty in the rms radius (a change in the rms radius of 1% will change the spectroscopic factor by 10%), and the fact that there might be some strength above 7 MeV excitation energy.

5. Conclusions

In this experiment we have deduced spectroscopic factors from the ^{51}V(d, ^{3}He)^{50}Ti reaction. The effects of the choice of different OM parameter sets for the d and ^{3}He were investigated as well as the effects of non-locality and finite-range corrections in the local energy approximation. The greatest uncertainty was found to originate from the prescription used for the BSWF. DWBA calculations indicate that the (d, ^{3}He) reaction probes only the exponential tail of the BSWF, which for a given spectroscopic factor, i.e. overall normalization, is rather sensitive to especially the rms radius of the calculated BSWF. Two methods were used for generating the BSWF, the fixed geometry method and the constant rms method, which result in two different sets of spectroscopic factors. It seems to us that the rms method is

preferable, because it yields relative spectroscopic factors for the 0^+, 2^+, 4^+ and 6^+ states in good agreement with those deduced from the (e, e'p) reaction, and because the radius of the binding potential increases with spin as expected (see sect. 3) from the arguments of Pinkston and Satchler [11]).

Notwithstanding the large uncertainties, which should be attributed to absolute spectroscopic factors, one can draw some conclusions on the fragmentation of the $l=0$, $l=2$ and $l=3$ strength. Most of the $l=3$ strength is contained in the ground state quadruplet, as found earlier [2,3]), but there is also a large number of small peaks above 4 MeV. The distribution of strength over the ground state quadruplet is very close to the simple shell-model prediction. Most of the $l=0$ strength can be found in the 3^- and 4^- levels at 4.409 and 6.041 MeV, but there are a few more levels containing about 10% of the $l=0$ strength. The $l=2$ strength is far more fragmented than reported earlier [2-5]). Due to the good resolution obtained in the present experiment, we were able to resolve some of the peaks observed in the earlier work [2,3]) into doublets. This will prove useful in the analysis of the (e, e'p) data, which were taken with worse resolution.

The absolute spectroscopic factors obtained in this work are much smaller than obtained earlier [2-5]), although the relative spectroscopic factors of the various experiments are in agreement with each other. The reason for this is that we have used a different BSWF and a non-local finite-range DWBA calculation, whereas the earlier work was analysed in local zero-range.

The results of the extensive shell-model calculation for the $1f_{7/2}$ pick-up strength to the low-lying quadruplet of states in ^{50}Ti are larger than our experimental values (again listed in table 7) and certainly much larger than the results deduced from the (e, e'p) experiment [1]) (see table 5). This indicates that if the experimentally observed depletion is realistic, our used basis is too restricted to reproduce the observed depletion which must then be occurring by removing strength to higher excitation energies where it is difficult to disentangle it experimentally.

However, we point out that the deduced spectroscopic factors from our (d, ^{3}He) experiment can be in rather good absolute agreement with the shell-model calculations if the rms radius for the $1f_{7/2}$ orbit turns out to be smaller than deduced from the (e, e') [ref. [20])] and (e, e'p) [ref. [1])] reactions. Of course, there remains then the disagreement with the absolute spectroscopic factors deduced from the (e, e'p) reaction. The origin of this disagreement will have to be sought elsewhere.

This work is part of the research program of the Stichting voor Fundamenteel Onderzoek der Materie (FOM) made possible by financial support from the Nederlandse organisatie voor zuiver Wetenschappelijk Onderzoek (ZWO).

References

1) J.W.A. den Herder, J.A. Hendriks, E. Jans, P.H.M. Keizer, G.J. Kramer, L. Lapikás, E.M. Quint, P.K.A. de Witt Huberts, H.P. Blok and G. van der Steenhoven, Phys. Rev. Lett. **57** (1986) 1843

2) F. Hinterberger, G. Mairle, U. Schmidt-Rohr, P. Turek and G.J. Wagner, Z. Phys. **202** (1967) 236

3) E. Newman and J.C. Hiebert, Nucl. Phys. **A110** (1968) 366
4) K. Ilakovac, L.G. Kuo, M. Petravić, I. Šlaus, P. Tomaš and G.R. Satchler, Phys. Rev. **128** (1962) 2739
5) J.N. Craig, N.S. Wall and R.H. Bassel, Phys. Rev. Lett. **36** (1976) 656
6) A. Moalem and Z. Vardi, Nucl. Phys. **A332** (1979) 195
7) A.G. Drentje, H.A. Enge and S.B. Kowalski, Nucl. Instr. Meth. **122** (1974) 485
8) J.C. Vermeulen, J. van der Plicht, A.G. Drentje, L.W. Put and J. van Driel, Nucl. Instr. Meth. **180** (1981) 93
9) H.P. Blok, J.C. de Lange and J.W. Schotman, Nucl. Instr. Meth. **128** (1975) 545
10) H.P. Blok, L. Hulstman, E.J. Kaptein and J. Blok, Nucl. Phys. **A273** (1976) 142
11) W.T. Pinkston and G.R. Satchler, Nucl. Phys. **72** (1965) 641
12) T. Berggren, Nucl. Phys. **72** (1965) 337
13) C.F. Clement, Phys. Lett. **28B** (1969) 398
14) C.F. Clement, Nucl. Phys. **A213** (1973) 469
15) C.F. Clement, Nucl. Phys. **A213** (1973) 493
16) P.D. Kunz, private communication
17) R.C. Johnson and P.J.R. Soper, Phys. Rev. **C1** (1970) 976
18) G.R. Satchler, Phys. Rev. **C4** (1971) 1485
19) A.E.L. Dieperink and I. Sick, Phys. Lett. **109B** (1982) 1
20) S.K. Platchkov, J.B. Bellicard, J.M. Cavedon, B. Frois, D. Goutte, M. Huet, P. Leconte, P.X. Ho, P.K.A. de Witt Huberts, L. Lapikás and I. Sick, Phys. Rev. **C25** (1982) 2318
21) R.H. Bassel, Phys. Rev. **149** (1966) 791
22) C.F. Clement and S.M. Perez, Nucl. Phys. **A284** (1977) 469
23) P.J. Brussaard and P.W.M. Glaudemans, Shell model applications in nuclear spectroscopy (North-Holland, Amsterdam, 1977)
24) K. Lips and M.T. McEllistrem, Phys. Rev. **C1** (1970) 1009
25) J.C. van der Merwe, Ph.D. thesis, University of Stellenbosch, 1974 (unpublished), quoted in ref. 5
26) M.L. Rustgi, R.P. Singh, B. BarmanRoy, R. Raj and C.C. Fu, Phys. Rev. **C3** (1971) 2238
27) T. Kuo and G.E. Brown, Nucl. Phys. **A114** (1968) 241
28) T.S. Sandhu and M.L. Rustgi, Phys. Rev. **C12** (1975) 666
29) R.B.M. Mooy and P.W.M. Glaudemans, Z. Phys. **A312** (1983) 59
30) R.B.M. Mooy and B.H. Wildenthal, private communication
31) L. Zybert, P.W.M. Glaudemans, R.B.M. Mooy and D. Zwarts, Z. Phys. **A318** (1984) 363
32) D.E. Alburger, Nuclear data sheets **42** (1984) 369
33) A. Yokoyama and H. Horie, Phys. Rev. **C31** (1985) 1012